Available online at www.sciencedirect.com

SciVerse ScienceDirect

Ceramics International 38 (2012) 5783–5789

CERAMICS INTERNATIONAL

www.elsevier.com/locate/ceramint

Synthesis of nanocrystalline cerium oxide by high energy ball milling

T.P. Yadav [a,b,*], O.N. Srivastava [b]

[a] Surface Science Research Centre and Department of Physics, The University of Liverpool, Liverpool L69 3BX, United Kingdom
[b] Centre of Advance Studies, Department of Physics, Banaras Hindu University, Varanasi 221005, India

Received 20 February 2012; received in revised form 7 April 2012; accepted 8 April 2012
Available online 16 April 2012

Abstract

We have synthesized pure nanocrystalline CeO_2 powders of nearly spherical shape using high-energy attritor ball mill. Milling parameters such as the milling speed of 400 rpm, ball to powder ratio (40:1), milling time (30 h) and water cooled media were determined to be suitable for synthesizing nanosize (~10 nm) powders of CeO_2. The powders after milling for various durations (up-to 50 h) were characterized by X-ray Diffraction, Scanning Electron Microscopy, Energy-dispersive X-ray Spectrometry and Transmission Electron Microscopy. An average particle size of 10 nm was obtained at 30 h milling, after which the particle agglomeration started, and a mixture of nanocrystalline and amorphous phase was observed after 50 h milling.

Keywords: Cerium dioxide; Ball milling; Catalysis; Nanocrystalline materials

1. Introduction

Oxides of rare earth elements are used widely in the catalyst industry to improve activity, selectivity and thermal stability. Cerium dioxide (ceria, CeO_2) has been widely investigated in recent years since it is a promising material for number of applications and therefore, holds particular significance amongst the rare earth oxides [1,2]. For example, CeO_2 is becoming an important material constituent in various fields of modern technology, such as catalysis, microelectronics, optoelectronics, electrochemical devices and ultraviolet blockers [3–5]. Also, the ability of cerium oxide to interact with phosphate ester bonds of biologically relevant molecules has important implications for their use as potential therapeutics [6]. The microstructure dependent physical properties have been studied in thin films of CeO_2 [7,8]. The shape dependent sensing properties of CeO_2 have been reported and this provides a new application of CeO_2 dendrites [9]. The ultrafine nm-sized particles of CeO_2 have attracted much attention since these particles often exhibit physical and chemical properties that are significantly different from those of bulk materials [10]. These CeO_2 ultrafine (~3 nm) particles have been prepared by solid-state reactions at room temperature [10]. The grain-size-dependent electrical conductivity of cerium oxide has been analyzed experimentally as well as theoretically using the space charge model for ionic solids [11]. Several processing routes including spray pyrolysis, microwave assisted thermal decomposition, electro synthesis, gas condensation, hydrothermal technique, homogeneous precipitation and flux methods have been investigated to synthesize nano-sized cerium dioxide powders [12–18]. The synthesis of ultrafine cerium dioxide (CeO_2) powders by anhydrous $CeCl_3$ and NaOH powders, along with NaCl diluent *via* mechanochemical reaction and subsequent calcination has been reported [19]. Recently, nanocrystalline CeO_2 samples were synthesized by a nonaqueous sol–gel method and their surface and interfacial areas were determined from nitrogen adsorption [20]. Considerable effort has been invested in order to produce nano-materials by mechanical milling/alloying [21]. This process has emerged as a popular method because of the possibility of producing large quantities of powders by repeated welding, fracturing and re-welding of powder particles subjected to high energy [22,23]. It is difficult to synthesize nano-size CeO_2 powders by mechanical milling because of the tendency of nanoparticles to form agglomerates during milling [24]. Nevertheless, some efforts have been made to synthesize nano-sized CeO_2 powder by mechanical milling [25,26]. Also, nano-composite powders of CeO_2/Zn

* Corresponding author.
E-mail addresses: yadavtp@gmail.com, t.yadav@liv.ac.uk (T.P. Yadav).

0272-8842/$36.00
http://dx.doi.org/10.1016/j.ceramint.2012.04.025

have been prepared with high-energy ball milling where corrosion resistance, hardness and uniformity of metal structure were improved significantly by encorporating nano-CeO_2 [27]. High-energy ball milling was found as a new process for the synthesis of pure gadolinium-doped ceria solid solution with homogenous microstructure and very fine particles containing nanocrystallites in the range of ~50 nm [28].

In the present work nanocrystalline cerium oxide powder has been synthesized by high energy ball milling. Nano-sized ceria particles have been produced after 30 h milling of as-received cerium powders of the micron size using ball milling technique.

2. Experimental procedures

The cerium (Ce) powders from Alfa Aesar with 99.6% purity and average particle size of ~5 μm, were used as starting material. A high-energy attritor ball mill (Szegvori attritor) was employed for mechanical ball milling (BM) with a ball to powder ratio of 40:1. The attritor has a cylindrical stainless steel tank of an inner diameter of 13 cm. The angular speed of the milling was maintained at 400 rpm and the milling operation was conducted from 10 to 50 h in dry (air atmosphere) medium. All the milling experiments were performed under chilled water-cooling system. The milled powder was characterized by X-ray diffraction (XRD) with CuK_α (λ = 1.5402 Å) radiation using Philips 1710 X-ray diffractometer. Structural and microstructural characterizations of mechanically milled powders were performed using a FEI: Technai 20 G^2 transmission electron microscope (TEM) at 200 kV. The elemental analysis was done using energy dispersive X-ray (EDX) attached to a QUANTA scanning electron microscope (SEM) operating at 20 kV.

3. Results and discussion

The typical XRD patterns of CeO_2 as a function of milling time are shown in Fig. 1(a–e). All the peaks have been indexed with cubic structure (fluorite type) of CeO_2 with a lattice parameter of, a = 5.42 Å. The fluorite structure of cerium oxide was not affected by ball milling. However, the degree of crystallinity decreased at higher milling times (after 30 h). The XRD peaks (Fig. 1(b–e)) became broader after milling, indicating that formation of nano-sized CeO_2 occurs as a result of milling after 20 h. The intensities of XRD peaks were observed to decrease with milling time. However, no additional peaks corresponding to any new phase were observed up to 50 h of milling indicating high purity of the final products. After 50 h of milling, peak broadening appeared in the XRD pattern at around 34°, which suggests amorphous phase formation together with nano CeO_2. The XRD pattern of 20–40 h of milling (Fig. 1(b–d)) clearly indicates that the (1 1 1) diffraction peak of CeO_2 phase is considerably broadened after ball milling, suggesting that nano-crystalline phase appears as a result of milling. The crystalline sizes of milled powders are found to decrease with milling time. The crystalline size and the lattice strain of the sample can be

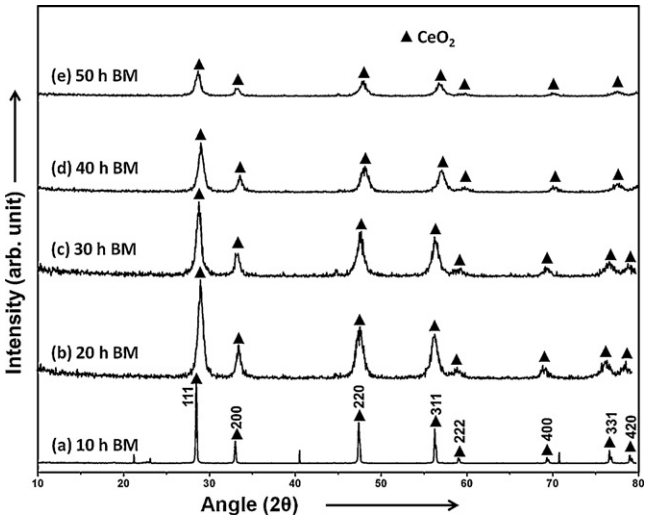

Fig. 1. The typical X-ray diffraction patterns of CeO_2 as a function of milling time (a–e). After 20 h of ball milling curve '*b*' indicates the formation of nanocrystalline type phase.

calculated from the integral width of the physical broadening profile. Cauchy and Gaussian components can be obtained from the ratio of full width at half maximum intensity (2ω) and integral breadth (β) [29]. In a single line analysis the apparent crystallite size 'D' and strain 'e' can be related to Cauchy (βc) and Gaussian (β_G) widths of the diffraction peak at the Bragg angle θ;

$$D = \frac{k\lambda}{\beta c \cos\theta} \tag{1}$$

and

$$e = \frac{\beta_G}{4\tan\theta} \tag{2}$$

The constituent Cauchy and Gaussian components can be given as

$$\beta_c = (a_0 + a_1\psi + a2\psi_2)\beta$$

$$\beta_G = (b_0 + b_{1/2}(\psi - 2/\pi)_{1/2} + b_1\psi + b_2\psi 2)\beta$$

where a_0, a_1 and a_2 are Cauchy constants, b_0, $b_{1/2}$, b_1 and b_2 are Gaussian constants and $\psi = 2\omega/\beta$ where β is the integral breadth obtained from XRD peak. The values of Cauchy and Gaussian constant have been taken from the table of de Keijser et al. [30]: a_0 = 2.0207, a_1 = 0.4803, a_2 = 1.7756; b_0 = 0.6420, $b_{1/2}$ = 1.4187, b_1 = 2.2043, b_2 = 1.8706. From these, we have calculated the crystallite size D and the lattice strain 'e' for the milled powder.

The overall variation of crystallite size, lattice strain and lattice parameter with milling time of CeO_2 nano particle are shown in Table 1. The lattice strain of CeO_2 initially increases up to 0.80% after 30 h of milling and thereafter decreases to 0.52% after 50 h. From this table it is clear that the crystallite size of CeO_2 decreases at a faster rate during initial milling times and then goes down at a relatively slower rate to finally attain a size of ~8 nm during milling operation. It is interesting to note that the lattice parameter is also found to increase during

Table 1
Crystallite size, lattice strain and lattice parameter of the CeO_2 with respect to milling time.

S.No.	Milling time (min)	Crystallite size (nm)	Lattice strain (%)	Lattice parameter (Å)
1	10	127	0.76	5.4201
2	20	53	0.79	5.4214
2	30	12	0.80	5.4236
3	40	11	0.69	4.4256
4	50	8	0.52	5.4289

milling. This indicates that relaxation of crystal structure in nanoscale morphology is responsible for an increase in the lattice parameter (Table 1).

Fig. 2 shows SEM images of the as-received and ball milled Ce powder. Fig. 2(a) reveals that as-received Ce crystallites are of micrometer sizes with arbitrary shape. Fig. 2(b) shows the 30 h ball milled CeO_2 powder with agglomerated morphology and this type of microstructure was found to be uniform throughout. A uniform small grain distribution can be seen in the dense microstructure. Energy dispersive X-ray (EDX) analysis with color mapping of 30 h BM CeO_2 has been shown in Fig. 3 which reveals that the contents are limited to Ce and oxygen only. It may be noticed that no other contamination like Fe, Cr or N has been detected. This could probably be due to the ice cooled ball milling experiment. The color mapping of EDX analysis shows homogeneous distributions of Ce and oxygen.

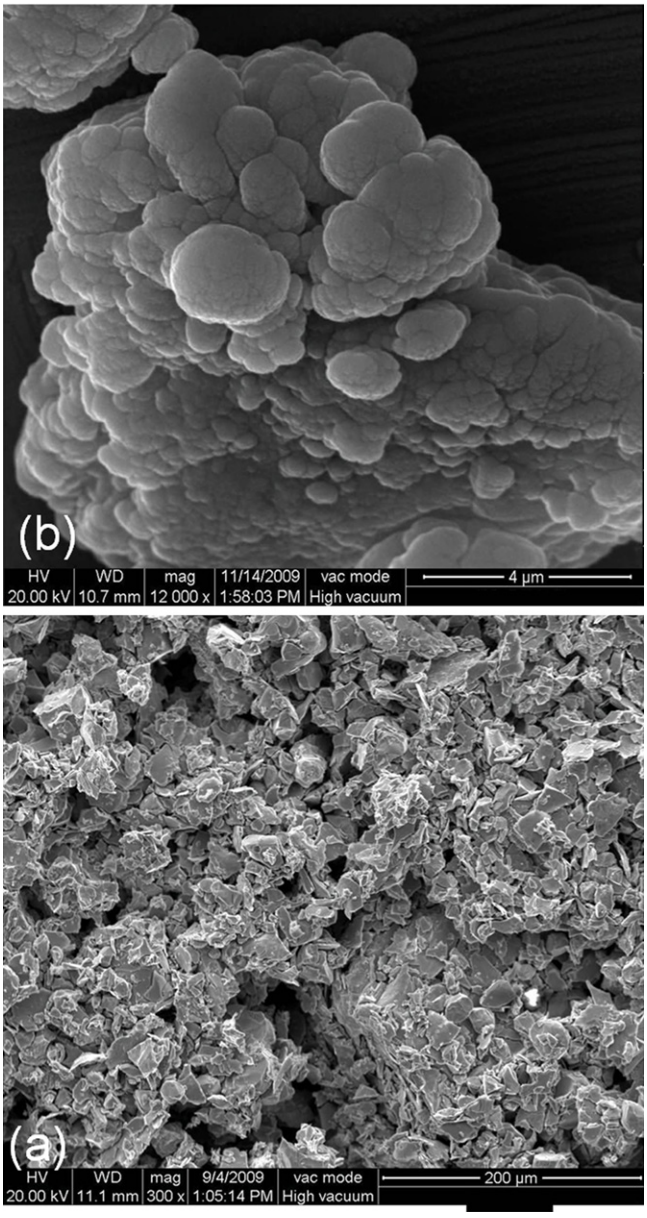

Fig. 2. (a) Scanning electron micrograph of as-received Ce, (b) CeO_2 after 30 h of ball milling under air atmosphere.

The nano-phase formation and milling effect was also confirmed by transmission electron microscopy. Fig. 4(a) shows a bright-field (BF) electron micrograph of 10 h BM CeO_2 powders. The grain sizes are found to vary from ∼150 to 200 nm. Fig. 4(b) shows a corresponding selected area electron diffraction (SAD) pattern which can be indexed based on face centered cubic (FCC) phase (a = 5.4 Å) along [0 0 1] zone axis. These features suggest the formation of disordered CeO_2 phase, which is in agreement with the XRD results. A typical TEM micrograph of the 30 h milled sample is shown in Fig. 4(c); from this, the average particle size of as-milled sample has been estimated to be ∼11 nm. The gray and white areas have been identified as different orientations in the nano-CeO_2 crystallites. The corresponding selected area electron diffraction pattern is shown in Fig. 4(d), which confirms the presence CeO_2 with a sharp spotty ring. The TEM micrograph of further milled (50 h) powder is shown in Fig. 4(e) and the corresponding SAD patterns in Fig. 4(f) are identified to be of the CeO_2 cubic phase. The crystallite/grain size distribution has been determined from 30 h BM CeO_2 BF TEM micrographs, showing an average grain size of ∼11 nm as shown in Fig. 5. The distribution of grain/crystallite sizes determined by TEM was normalized to unit area and standard deviation of the size distributions is calculated to be ∼3 nm. The histograms of crystallite size distribution shows a very narrow dispersion in the size of CeO_2 obtained in the present experimental conditions.

Fig. 6 shows a high-resolution transmission electron microscopy (HRTEM) image of the 30 h milled powders with the inset showing a Fourier transform (FFT) of the image. The HRTEM clearly exhibit a nanometric granular microstructure with lattice resolution. Typically, grains are rounded with sizes between 8 and 12 nm, and no significant through-thickness variations are observed. Careful inspection reveals that some crystals are oriented along the [0 0 1] direction indicated by an arrow. Simple inspection of their lattice images reveals that the grains are highly disorientated from each other. The lattice parameter is calculated by the crystallographic planes and it is close to the lattice parameter calculated by XRD. The HREM

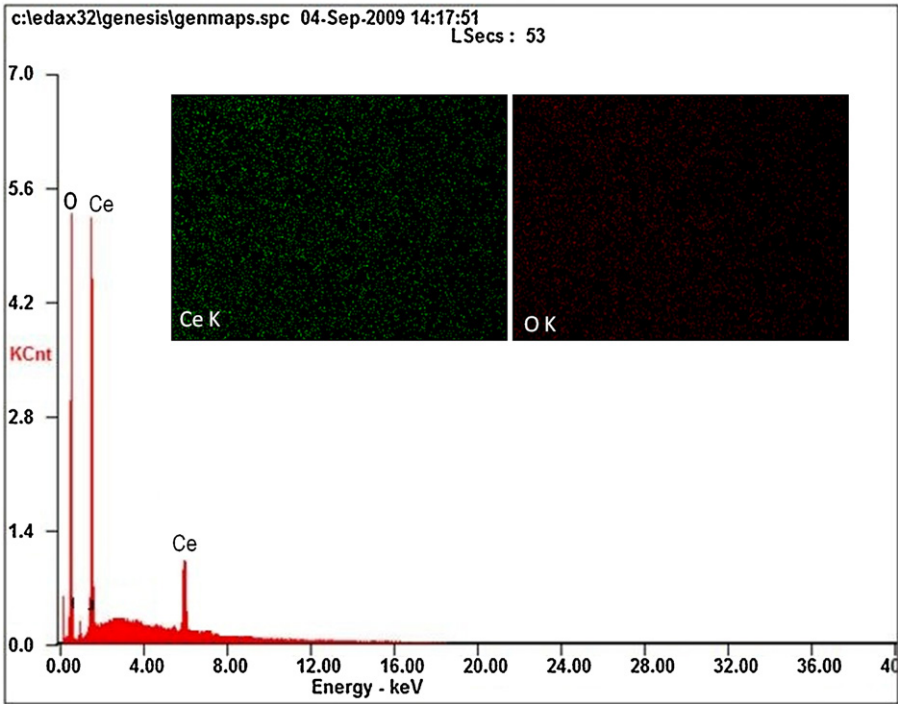

Fig. 3. Energy dispersive X-ray spectrum of the 30 h ball milled powder, showing the presence of the Ce and O elements only.

observation in this study indicates that CeO_2 prepared by high energy BM method consists of small crystallites with different crystallographic orientations separated by grain boundaries. The average grain size obtained from measuring more than 10 grains was about 10 nm. The HRTEM image of a typical area, which contains a number of grains and grain boundaries, is shown in Fig. 6. It can be seen that most of the grain boundaries of CeO_2 have ordered structures; however, the grain boundary facets are curved and coarse due to the strain induced during BM. Lattice fringes near the grain boundary are somewhat distorted, which indicates the presence of local strain in the grain boundary regions. However, HRTEM of longer BM (50 h) powder shows more disordered grain boundary regions in Fig. 6(b). In other words, CeO_2 consists of a crystalline matrix surrounded by amorphous type phases. It is also supported by the Fourier transform (inset of Fig. 6(b)) taken from region 'A'. From the HRTEM investigations, it is apparent that the amorphous phases in CeO_2 nanomaterials depend on the milling time. It can be concluded that, the 30 h BM can be considered as best milling time parameter for the synthesis of CeO_2 nano crystallites using the present synthesis method.

The experimental studies on the synthesis of nano-sized CeO_2 using high-energy ball milling technique have been reported [25–28]. The thermodynamic driving force is quite favorable for CeO_2 formation at room temperature during BM. However, previous studies have taken several elements/compounds as a precursor for the synthesis and the CeO_2 powders were not homogenous in size. In our present study, it was found that the mechanical milling of Ce in oxygen ambient results in the formation of CeO_2 in the initial stages of milling, *i.e.* at 10 h, and finally a nano-crystalline (∼10 nm) microstructure of CeO_2 is obtained after 30 h of BM. However, in further milling (40 h and 50 h) amorphous layers around the CeO_2 crystallites have been observed. Therefore, it is clear from above observation that the longer milling times are not favorable for the synthesis of homogenous nano-crystalline CeO_2. It seems that the grain refinement during the initial stages of milling (up to 10 h BM) is accompanied by oxidation of Ce while further milling results in grain reduction only. This can be inferred from the XRD profile, where the broadening as well as weakening of the XRD peaks is observed with the increasing milling time, as shown in Fig. 1. These results may be associated with enhanced dislocation density and CeO_2 formation in addition to grain size reduction. From the X-ray diffraction patterns, it is evident that the formation of disordered CeO_2 can be achieved by high energy BM alone. At the initial stage of milling, *i.e.* 20 h BM, the disordered CeO_2 phase contains large amount of defects and grain boundaries resulting in considerable strain. Therefore additional milling treatment is necessary to allow the system to attain a mechanical and statistical equilibrium. Here further milling is sufficient to reduce the defects leading to strain-relaxation. However, small amounts of strain have been observed in even longer milling periods as can be seen in Table 1. It should be pointed out that all the strain cannot be fully removed by mechanical milling and post annealing alone as other equilibration processes are critical steps to obtain strain-free nano-phases [31]. Another effect related to the reduced size of the crystallites as well as oxide phase formation under our present experimental conditions might be due to cooling. The whole milling chamber is a chilled water-cooled system. Due to

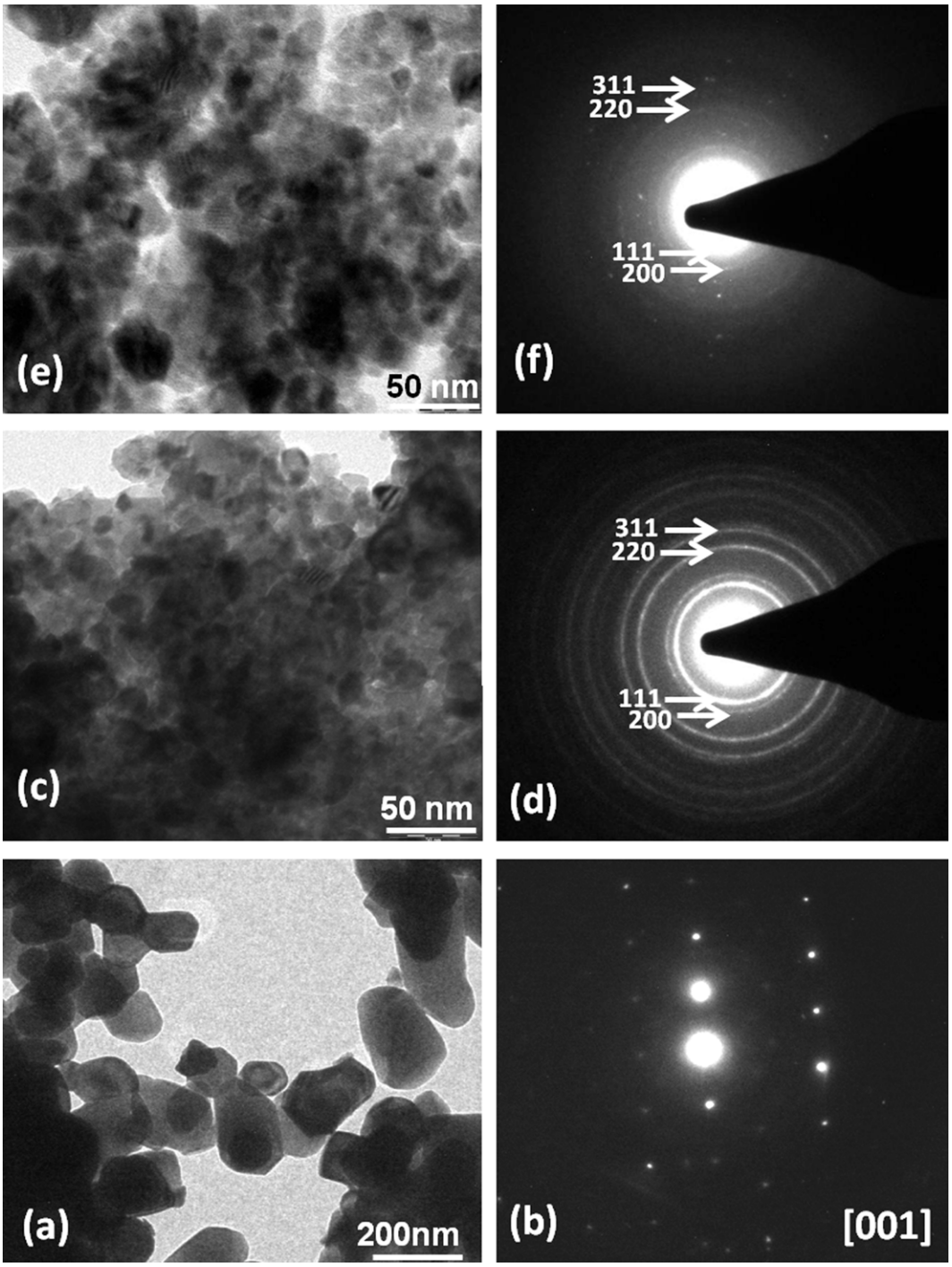

Fig. 4. (a) Bright field TEM image of as-received CeO_2, (b) corresponding SAD pattern, (c) bright field TEM image of 30 h BM, (d) corresponding SAD pattern, (e) bright field TEM of 50 h BM, (f) corresponding SAD pattern.

the Gibbs–Thomson effect, the solubilities of solutes are expected to be enhanced in solid solution, with grain refinement down to the nanometer regime [29]. In the nanocrystalline state, solute atoms are known to segregate to the boundaries forming a solute cloud in the vicinity of the boundaries. Therefore, the solid solubility in the grain boundaries may differ considerably from that in the interior of the crystal. During further milling in presence of metastable CeO_2 phase solid solution, nucleation processes leading to stable single-phase formation of CeO_2 may take place under appropriate thermodynamic conditions. We would also like to point out that due to the formation of nano sized Ce during the very initial stages of milling; there is a possibility of significant surface diffusion, which would enhance the oxidation of Ce. However, it must be emphasized that there is a need for further study to confirm the sequence of the CeO_2 formation during high-energy ball milling.

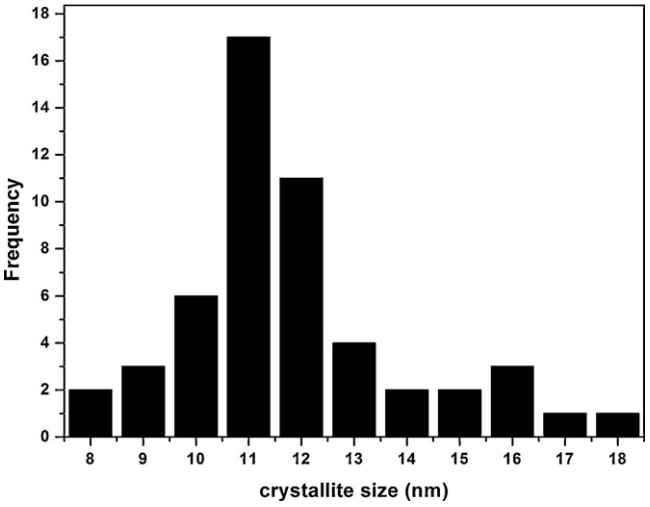

Fig. 5. Histograms of crystallite size distribution measurements by TEM microstructure performed on powders ball milled for 30 h. The standard deviation of the size distributions is 2.5.

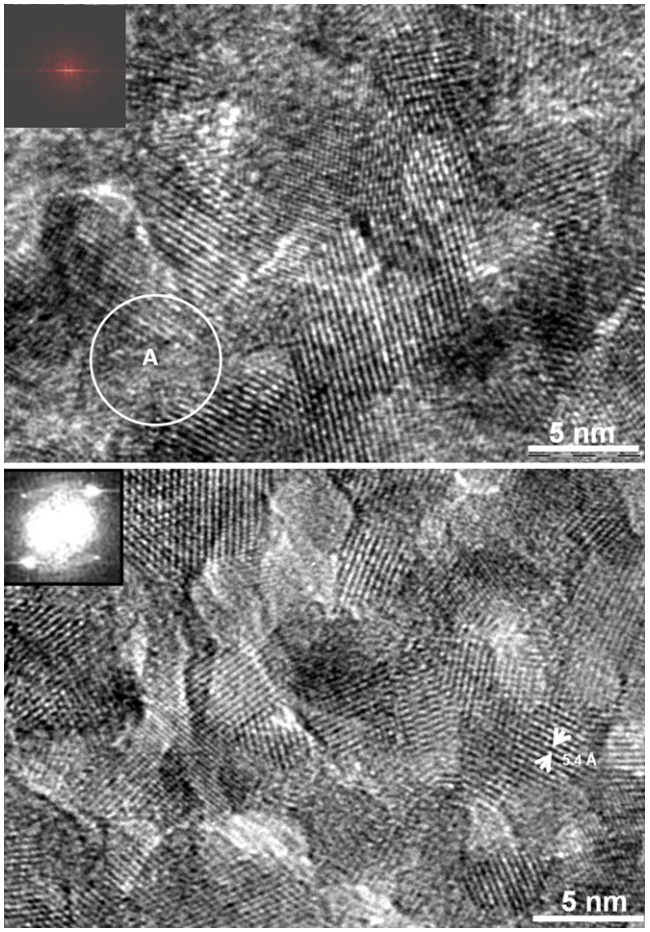

Fig. 6. High-resolution TEM image of a 30 h ball milled CO_2 particle. The white arrows indicate edge dislocations. The extra plane of atoms can be seen by viewing along the direction indicated by arrows.

4. Conclusion

We have successfully synthesized nano sized CeO_2 powder by high energy ball milling. The structural and microstructural investigation reveals the formation of pure and defect free CeO_2 nanoparticle which are nearly of spherical shapes of about 10 nm size. The optimum milling time was determined to be 30 h under ice cooled milling atmosphere. The CeO_2 are uniformly distributed and randomly oriented with ultrafine crystallites.

Acknowledgements

The authors would like to thank Prof. R.S. Tiwari, Prof. N.K. Mukhopadhay, Prof. B.S. Murty and Dr. M.A. Shaz for their keen interest and useful discussions. The authors would also like to thank G. Irene Sheeja for supplying useful references and stimulating discussions. We would like to thank Dr. V.S. Subrahmanyam and D.K. Rai for a critical reading of the manuscript and valuable suggestions. TPY thanks the Department of Science and Technology (DST) for BOYACAST fellowship during which period a part of the work was completed. The financial support of the DST and Ministry of New and Renewable Energy, India is gratefully acknowledged for carrying out this work.

References

[1] S. Singh, T. Dosani, A.S. Karakoti, A. Kumar, S. Seal, W.T. Self, A phosphate-dependent shift in redox state of cerium oxide nanoparticles and its effects on catalytic properties, Biomaterials 32 (2011) 6745–6753.
[2] C.C. Chuang, M.J. Chen, H.I. Hsiangw, F.S. Yen, Effect of Ba21 addition on phase separation and oxygen storage capacity of $Ce_{0.5}Zr_{0.5}O_2$ powder, Journal of American Ceram Society 94 (3) (2011) 895–901.
[3] P.C.C. Faria, D.C.M. Monteiro, J.J.M. Órfão, M.F.R. Pereira, Cerium, manganese and cobalt oxides as catalysts for the ozonation of selected organic compounds, Chemosphere 74 (2009) 818–824.
[4] P.M. Shibli, S.M.A. Ashraf, Development of cerium oxide and nickel oxide-incorporated aluminium matrix for marine applications, Journal of Alloys and Compounds 484 (2009) 477–482.
[5] D.O. Raemy, L.K. Limbach, B.R. Rutishauser, R.N. Grass, P. Gehr, K. Birbaum, C. Brandenberger, D. Günther, W.J. Stark, Cerium oxide nanoparticle uptake kinetics from the gas-phase into lung cells in vitro is transport limited, European Journal of Pharmaceutics and Biopharmaceutics 77 (2011) 368–375.
[6] M.H. Kuchma, C.B. Komanski, J. Colon, A. Teblum, A.E. Masunov, B. Alvarado, S. Babu, S. Seal, J. Summy, C.H. Baker, Phosphate ester hydrolysis of biologically relevant molecules by cerium oxide nanoparticles, Nanomedicine: NanotechnologyBiology, and Medicine 6 (2010) 738–744.
[7] T. Suzuki, I. Kosacki, H.U. Anderson, P. Colomban, Electrical conductivity and lattice defects in nanocrystalline cerium oxide thin films, Journal of American Ceram Society 84 (9) (2001) 2007–2014.
[8] I. Kosacki, V. Petrovsky, H.U. Anderson, P. Colomban, Raman spectroscopy of nanocrystalline ceria and zirconia thin films, Journal of American Ceram Society 85 (11) (2002) 2646–2650.
[9] D. Zhang, W. Wu, X.J. Ni, X.Y. Cao, X.B. Zhang, X.Y. Xu, S.Z. Li, G.Q. Han, A. Ying, Z.W. Tong, Fabrication and characterization of novel bowknot-like CeO_2 crystallites and applications for methyl-orange sensors, Journal Material Science 44 (2009) 3344–3348.
[10] X. Yu, F. Li, X. Ye, X.X.Z. Xue, Synthesis of cerium(IV) oxide ultrafine particles by solid-state reactions, Journal of American Ceram Society 83 (4) (2000) 964–966.
[11] A. Tschope, S. Kilassonia, B. Zapp, R. Birringer, Grain-size-dependent thermo power of polycrystalline cerium oxide, Solid State Ionics 149 (2002) 261–273.

[12] T. Masui, H. Hirai, N. Imanaka, G. Adachi, Synthesis of cerium oxide nanoparticles by hydrothermal crystallization with citric acid, Journal of Materials Science Letters 21 (2002) 489–491.
[13] M.S. Tsai, Powder synthesis of nano grade cerium oxide via homogenous precipitation and its polishing performance, Materials Science and Engineering B 110 (2004) 132–134.
[14] H. Gu, M.D. Soucek, Preparation and characterization of monodisperse cerium oxide nanoparticles in hydrocarbon solvents, Chemistry of Materials 19 (2007) 1103–1110.
[15] L. Gu, G. Meng, Powder synthesis and characterization of nanocrystalline CeO_2 via the combustion processes, Materials Research Bulletin 42 (2007) 1323–1331.
[16] A. Bumajdad, J. Eastoe, A. Mathew, Cerium oxide nanoparticles prepared in self-assembled systems, Advances in Colloid and Interface Science 147–148 (2009) 56–66.
[17] Q. Zhang, Z. Yang, B. Ding, Synthesis of cerium oxide nanoparticles by the precipitation method, Materials Science Forum 610–613 (2009) 233–238.
[18] I. López, T.V. Solís, G. Marbán, The synthesis of high surface area cerium oxide and cerium oxide/silica nanocomposites by the silica aquagel-confined co-precipitation technique, Microporous and Mesoporous Materials 127 (2010) 198–204.
[19] T. Tsuzuki, P.G. McCormick, Synthesis of ultrafine ceria powders by mechanochemical processing, Journal of American Ceram Society 84 (7) (2001) 1453–1458.
[20] S. Hayun, S.V. Ushakov, A. Navrotsky, Direct measurement of surface energy of CeO_2 by differential scanning calorimetry, Journal of American Ceram Society 94 (11) (2011) 3679–3682.
[21] T.P. Yadav, N.K. Mukhopadhyay, M.A. Shaz, R.S. Tiwari1, O.N. Srivastava, Formation of nano-quasicrystalline decagonal phase in the $Al_{70}Cu_{10-}Co_5Ni_{15}$ system by high energy ball milling, Journal of Nanoscience and Nanotechnology 9 (2009) 5527–5532.
[22] B.S. Murty, S. Ranganathan, Novel materials synthesis by mechanical alloying/milling, International Materials Review 43 (1998) 101–141.
[23] C. Suryanarayana, Mechanical alloying and milling, Progress in Materials Science 46 (2001) 1–184.
[24] A. Matraszek, I. Szczygie, L. Macalik, J. Hanuza, Mechanochemical synthesis of cerium orthophosphate, Journal of Rare Earths 27 (4) (2009) 598–602.
[25] A. Hadi, I.I. Yaacob, L.S. Ling, Mechanochemical synthesis of nanocrystalline CeO_2: the effect of annealing temperatures on the particle size, Materials Science Forum 517 (2006) 252–256.
[26] A.V. Chadwick, S.L.P. Savin, EXAFS study of nanocrystalline CeO_2 samples prepared by sol–gel and ball-milling routes, Journal of Alloys and Compounds 488 (2009) 1–4.
[27] W. Qian, Preparation and properties of nano-CeO_2/Zn composites, Transactions Nonferrous Metals Society of China 17 (2007) s622–s625.
[28] Z. Khakpour, A.A. Youzbashi, A. Maghsoudipour, K. Ahmadi, Synthesis of nanosized gadolinium doped ceria solid solution by high energy ball milling, Powder Technology 214 (2011) 117–121.
[29] T.P. Yadav, N.K. Mukhopadhyay, R.S. Tiwari, O.N. Srivastava, Studies on the formation and stability of nano-crystalline $Al_{50}Cu_{28}Fe_{22}$ alloy synthesized through high-energy ball milling, Materials Science and Engineering A 393 (2005) 366–373.
[30] Th.H. de Keljser, J.I. Langford, E.J. Mittemeijer, A.B.P. Vogels, Use of the Voigt function in a single-line method for the analysis of X-ray diffraction line broadening, Journal Applied Crystallography 15 (1982) 308–314.
[31] B. Bokhonov, M. Korchagin, Application of mechanical alloying and self-propagating synthesis for preparation of stable decagonal quasicrystals, Journal of Alloys and Compounds 368 (2004) 152–156.